Genetic Optimizations of EC-135 Noise Abatement Flight Procedures using an Aeroacoustic Database

Frédéric Guntzer, Pierre Spiegel, Markus Lummer

DLR in der Helmholtz Gemeinschaft,
Institute of Aerodynamics and Flow Technology, Technical Acoustics Division,
Lilienthalplatz 7, 38108 Braunschweig, Germany

Corresponding author: Frederic.Guntzer@dlr.de

Abstract

This paper describes the implementation of the DLR SELENE computation chain, able to predict the noise of an arbitrary flight, in a genetic optimizer and the resulting optimization of noise abatement landing procedures for the EC135 helicopter. At each iteration of an optimization, a complete procedure noise footprint is calculated starting from way points prescribing the position and velocity of the helicopter. The noise simulation relies on the use of a database of noise directivity versus flight conditions, in the present case resulting from 2004 flight tests. The optimizer then adjusts the way points in order to minimize the noise on ground. Procedures that do not satisfy safety, comfort and flyability constraints are rejected. A series of such optimizations has been launched and exhibits some trends. The confrontation of each optimized procedure to a torque/velocity diagram shows the relevance of the already observed torque-noise correlation. It seems that the optimized procedures are quite robust to side wind and helicopter mass variations. On the contrary, a headwind component has a clear impact on the optimized procedures and on their noise footprint. Several optimized procedures were validated during flight tests in 2008. A good agreement between simulated and measured noise levels is observed. The flight tests confirm the predicted noise reduction by 10 dB SEL between 3 km and 1 km before the landing point. The optimized flight procedures are evaluated as well flyable. A modification of the helicopter fin would make them completely comfortable.

Notation

Exhaustive definitions of the variables used at DLR and in some EU Projects, and in particular for this study, relating to helicopter dynamics, aerodynamics and acoustics are provided in [1] which is available at www.dlr.de/Friendcopter-dictionary. We list here only the variables and abbreviations used in this paper.

Name	Symbol	Signification
NAFP		Noise Abatement Flight Procedure.
S	*S*	Simulation coordinate system, fixed with respect to ground.
H	*H*	Helicopter coordinate system.
HO	*HO*	Reference point of the helicopter.
HO_Si	*HO_Si*	Position of HO along i[th] component of S.

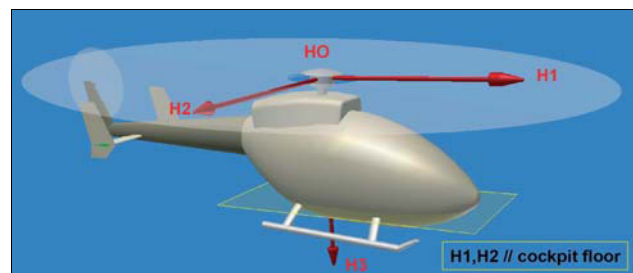*Fig. 1: Axes (H1,H2,H3) and reference point (rotor head center of the main rotor, HO) of the helicopter coordinate system (H).*

VHO_Si	VHO_Si	component along Si of the velocity of HO with respect to ground.
NormVHO_S	$\left\vert VHO_S \right\vert$	Norm of HO velocity. with respect to ground.
psi	ψ	Helicopter heading angle.
theta	θ	Helicopter pitch angle.
phi	ϕ	Helicopter roll angle.
alpha	α	Fuselage angle of attack.
beta	β	Side slip angle.
gamma	γ	Path angle with respect to ground.
ETorqueNom	T_{EN}	Engine nominal torque (*i.e* corresponds to 100 % torque ratio).
EOmega	Ω_E	Engine(s) rotation speed.
PmAlpha	α_{P_m}	Main rotor tip path plane angle of attack.
RmCT	CT_{R_m}	Main rotor thrust coeff.
RmMu	μ_{R_m}	Main rotor advance ratio.
RmOmega	Ω_{MR}	Main rotor rotation speed.
RmTorque	T_{MR}	Main rotor torque (positive when rotor is driven by engine).
RtOmega	Ω_{TR}	Tail rotor rotation speed.
RtTorque	T_{TR}	Tail rotor torque.
sigma	σ	Ground flow resistivity.

Introduction

This paper focuses on noise abatement flight procedure optimization for helicopters. For helicopter manufacturers and operators, the helicopter noise perceived on ground is a major concern because it reduces the public acceptance of helicopters and hence their operation field and market. This noise problem can be alleviated by designing new helicopters (for instance through purposeful blade design or active blade control), or by designing flight procedures which minimize the noise perceived on ground. The helicopter group of the technical acoustic division of DLR has been involved in the second strategy for several years. Flight test campaigns and projects have been dedicated to progress on this topic as reported in [2], [3], [4], [5] and [6]. Attempts have been made in designing noise abatement flight procedures by modeling them as a series of steady flight segments [3]. But this method does not account for the large impact on noise emission of the transition between segments and of the necessary maneuvering conditions such

as acceleration or deceleration. In the present approach the flight are considered as maneuvering flights and a corresponding noise emission model is used. As there is an infinity of possible flight procedures between two geometrical points, a parametric investigation only by hand would be limited. Therefore, in the present approach the implementation and use of an automatic optimization process has been selected. An important aspect in the acoustic evaluation of helicopter flight procedures is the consideration of wind, wind gradients and mass, which varies from one flight to another. Indeed, all these aspects have an impact either on the noise emission or on its propagation to the ground and should be considered. Moreover, the designed flight procedures must be flyable, safe and should be comfortable.

This paper presents the optimization process, developed at DLR, aiming to design flight procedures minimizing the noise perceived on ground. Although, the method is applicable to any kind of flight procedure, we focus here on landing approaches as they represent currently the most annoying flight phase. All the applications and validation examples shown over the paper concern an EC135 helicopter.

We first recall how we simulate a single arbitrary procedure noise footprint using the DLR SELENE computation chain, which is based on the use of a noise directivity database. The optimization loop is a coupling between SELENE and a commercial optimizer [7].

Then we explain how such a noise directivity database was constructed through dedicated EC135 flight tests.

The description of the optimization parametrization and setup follows then with considerations on flight parametrization, cost function, environment modeling, flyability constraints, optimization algorithm setting and CPU time versus convergence.

Resulting optimized landing procedures of an EC135 are then described with illustration of the effect of mass, wind, or changes in the optimization settings such as setting free the initial height.

Finally some results of validation flight tests are shown with comparison between simulation and flight and with the evaluation of the noise reduction achieved in flight.

In order to consider manufacturer interest to keep some helicopter characteristics confidential, the noise results shown in this paper are all amplified by a factor, being constant over the whole paper.

1. SELENE computation chain in forward propagation

This section describes the calculation of an arbitrary procedure noise footprint, *i.e.* how a single iteration of a noise abatement flight procedure optimization is managed. Indeed, one of the two main functionalities of the SELENE (stating for **S**ound **E**xposure **L**evel starting from the **E**mitted **N**oise **E**valuation) computation chain is to process such calculations. This is done using a database of noise directivity as function of flight conditions. Usually the directivity is expressed onto a sphere and represents the far-field noise spectra versus the observer direction relative to the helicopter. The database must cover a sufficiently wide range of flight conditions for a given helicopter. It can result indifferently from numerical simulations or from flight tests processing. This computation chain, although not already entitled as

"SELENE", was already described and verified in [5]. We will thus only here recall its main features.

Using SELENE to simulate an arbitrary procedure footprint is defined as the "forward propagation" functionality. Fig. 2 provides the flowchart (in UML2 activity diagram conventions) of the corresponding part of SELENE, embedded in the optimization loop of a commercial optimizer (ModeFrontier [7] is currently used for this study). Such a forward propagation calculation involves the following steps.

1.1. Flyable procedure generation

SELENE starts from a user- or optimizer- given set of way points (where positions and velocities with respect to ground are prescribed) to generate a 3D flight procedure smooth enough to be flyable by a helicopter with respect to flight mechanics. This is made in the following manner.
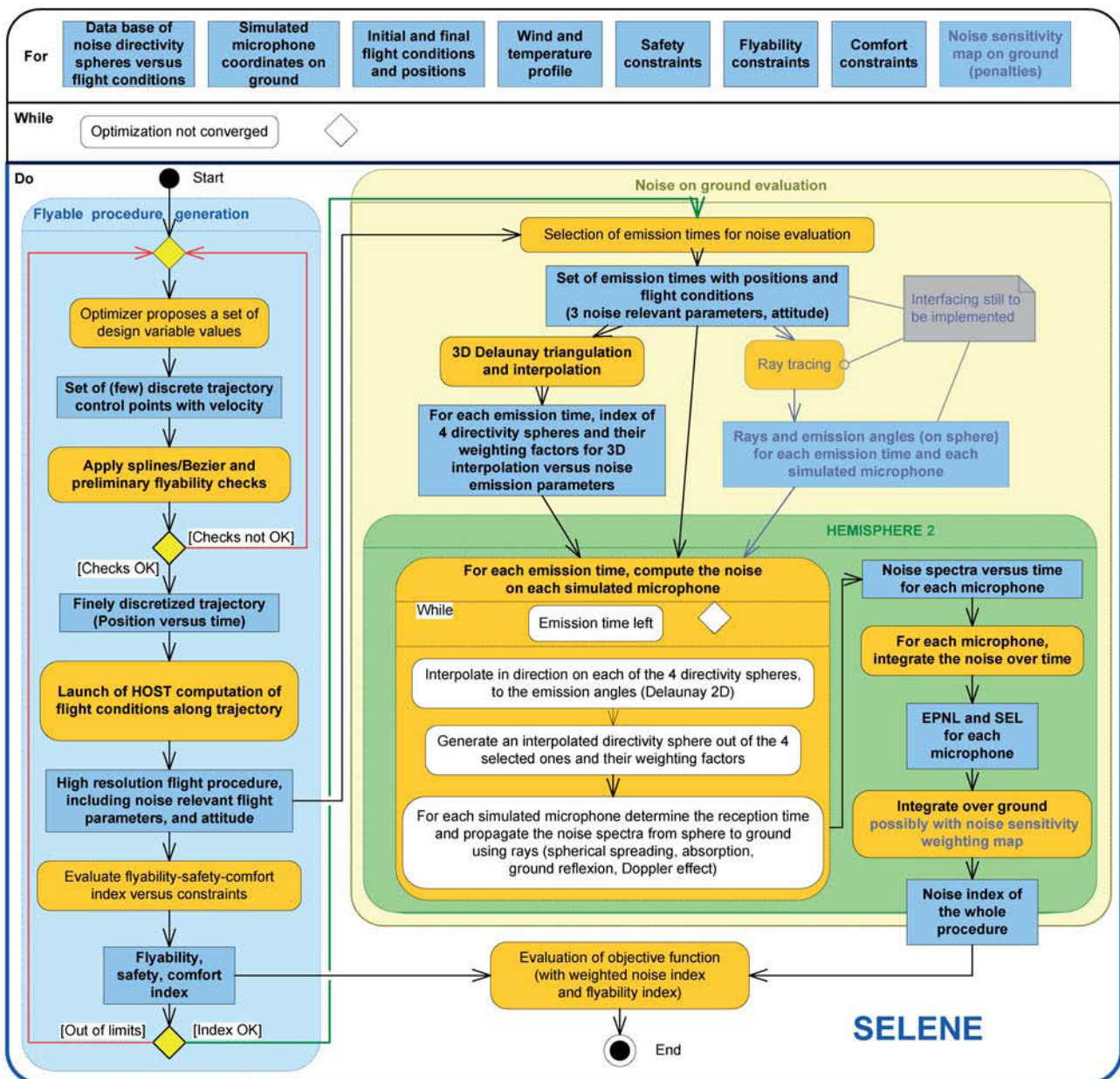

Fig. 2: Activity diagram of SELENE embedded in the optimization loop.

3

The flight path is approximated using cubic Bézier splines [8]. Smooth curves are obtained but the trajectory does not pass exactly through the way points. This, however, does not have negative consequences for the optimization procedure. The points are sometimes rather called "control points" than "way points" because the resulting procedure does not exactly cross them. In order to obtain the higher order derivatives of the path needed for the subsequent flight mechanics computation, the Bézier spline is then interpolated by ordinary cubic splines and the time is obtained by integration along the curve knowing the interpolated velocity at each point. For the calculation of the acceleration, a spline on spline approach is used, *i.e.* the velocity vector is again approximated by cubic splines and this approximation is differentiated. A slight disadvantage of use of the Bézier spline approach for procedure generation is that zero acceleration intervals can only be achieved approximately using a proper choice of the control points. However the obtained procedures were systematically smooth enough to be compatible with helicopter flight mechanics. Note that the flight procedure is for the moment only defined relative to the ground fixed coordinate system *S* and that the velocity of the helicopter relatively to the air depends also on the selected wind profile.

At this stage preliminary controls are performed such as the check that linear accelerations remain inside prescribed limits.

Next HOST, a helicopter flight dynamics program from Eurocopter (and partners) [9], simulates the flight along the generated trajectory (equilibrium calculation and inverse simulation) in order to determine the value of several "noise relevant flight parameters" (whose selection is explained in Section 1.3) and the helicopter attitude angles (determining the simulated noise directivity sphere attitude) along the procedure. Possible execution errors are managed automatically up to a certain extent. Note that at this step a vertical profile of wind velocity components is considered.

Flyability, safety and comfort checks that necessitate the flight dynamics evaluation are then performed: HV diagram compatibility, vortex ring state avoidance, acceleration time derivative within limits, remaining margin to autorotation, compatibility of the attitude with the pilot visibility in track and landing point directions. It is also possible to exclude procedures including values of *theta*, *gamma* or sink rate exceeding prescribed limits. All the flyability parameters implemented in the flyability module were defined with the participation of the DLR test pilots, especially after some preliminary flight tests of the first optimized procedures.

1.2. Evaluation of the noise on ground using HEMISPHERE 2

Finally, the calculation of the ground noise is performed using on the one hand the relevant flight parameters provided by HOST along the generated trajectory, and on the other hand, a data base of far-field noise directivity spheres. The database used up to now at DLR results from flight tests whose measured data have been processed using the so-called SELENE "backward propagation" functionality to construct the noise directivity spheres. In this backward propagation process the experimental data are corrected from the effects of the test conditions, such as wind, ground microphone setup directivity... (see [5] for the details of a spheres database construction).

A series of emission times for which the noise propagation to ground will be simulated is then selected (currently a constant time step of 1 second is used). At each emission time, the spheres in the database whose noise relevant flight parameters are the closest to the HOST-calculated flight parameters are identified. This is achieved thanks to a Delaunay triangulation of the flight parameters of all spheres in the database. The spheres are not only selected but their weighting is calculated so that the flight condition at the selected time results from the weighted average of the flight condition of the selected spheres.

Then the sound is propagated to the ground by the code HEMISPHERE 2. As the direction relative to the helicopter of the simulated ground microphones generally differs from the directions documented on the database spheres (corresponding to the flight-test ground microphones) a 2D interpolation (using also a Delaunay triangulation) is preliminarily performed on the selected database spheres to get the noise emission towards the simulated microphones. A simulated noise directivity sphere can then be interpolated from the selected and rearranged database spheres to represent the noise directivity of the helicopter corresponding to the flight parameters at the considered time. This is performed using the preliminarily set weighting. The propagation to the ground is then simulated considering following effects: Doppler effect, atmospheric absorption, spherical spreading and ground reflexion. As already suggested in gray in Fig. 2, the consideration of the wind and temperature gradients is still in preparation, and will be based on the interfacing of an existing ray tracing DLR code.

Once noise propagation for all selected emission times are processed, time-integrated noise metrics such as SEL, EPNL are computed and outputted. There are several way to define a noise characterizing a whole flight procedure starting from the evaluated noise levels on each simulated microphone. The most used up to now is the average SEL level on the ground surface covered by

4

simulated microphones.

1.3. Selection of noise relevant flight parameters

As announced previously the simulation chain using a noise directivity database relies on the assumption that the noise emission of a helicopter can be described as depending on a limited number of flight parameters, so that the noise emission for a given flight condition can be obtained interpolating along these parameters the available noise directivity spheres in the database. The number of parameters has to be kept relatively small because the number of noise directivity evaluations necessary to fill the database is rapidly increasing with the number of independent parameters. Note that we want here to simulate also maneuvering flights as they occur necessarily in real flight procedures and can have a high impact on noise emission. As the selection of noise relevant flight parameters has an impact on the definition of flight tests made to built a noise directivity database, it has been performed prior to such dedicated flight tests which occurred in 2004 (within the DLR PAVE project), and has already been explained in [4]. It is only briefly reminded here.

Many studies on helicopter noise, especially concerning the loud Blade Vortex Interaction (BVI) noise, and main rotor noise in general led to choose the three following aerodynamic parameters as the most influent on noise emission :

- α_{P_m} (*PmAlpha*) : the angle of attack of main rotor tip path plane

- CT_{R_m} (*RmCT*) : the lift coefficient of the main rotor

- μ_{R_m} (*RmMu*) : the advance ratio of the main rotor (with the assumption that the main rotor has a constant rotation speed).

In the present version of SELENE, and in the spheres database mentioned in this document, the flight conditions are characterized only by these 3 parameters, for maneuvering flight as well as for steady flights (as verified in [5]). Note that the widely used representation of noise emission versus horizontal and vertical velocities is only valid for steady flights.

As the selected noise emission parameters are mainly those of the main rotor, the noise emission direction should be measured relative to the tip path plane and flight direction relative to air. However it is assumed that the tip path plane attitude relative to the fuselage for a given set of the 3 chosen parameters does not significantly change between usual helicopter loadings (center of gravity position variations), and the noise emission direction is then rather expressed relative to the fuselage whose attitude relative to ground is given by the attitude angles *psi*, *theta*, *phi*. This is motivated by the fact that the fuselage attitude is usually measured and therefore well known, whereas the main rotor tip path plane is not measured but results from simulations whose models and results may evolve in future, which would need to reconstruct the spheres.

Another expected noise influent flight parameter is the side slip angle *beta*. However, performing an additional systematic investigation on beta, for each combination of the 3 previous selected noise relevant parameters was not possible within the time frame of the PAVE 2004 flight tests. Beta investigations in flight were performed but only for a reduced number of combinations of the 3 previous parameters. Therefore, with the resulting database, systematic noise noise evaluation (and consequently optimization) can only be performed for flights with nearly zero side-slip, and only those kind of flights are considered in the simulations/optimizations presented in this paper. Nevertheless, DLR flight tests in 2008 showed that the side slip angle *beta* can have a tremendous effect on avoidance of Fenestron noise increase occurring at high angle of attack of the main rotor (for example in steep descent or in deceleration) [6]. But, the same flight tests showed also that flight procedure optimized with the 3 above mentioned parameters as noise relevant flight conditions could benefit from Fenestron noise excess avoidance by additional side-slip without any main rotor noise increase. The consideration of only zero *beta* cases in the simulation seems therefore not penalizing.

2. Exploitation of PAVE 2004 flight tests

2.1. Construction of a sphere database

The previously described computational chain relies on the existence of a database providing the noise emission characteristics as function of flight conditions. Concerning the present EC135 optimizations, the database has been obtained through the PAVE 2004 flight tests. For an exhaustive description of these flight tests, see [4].

The aeroacoustic database associates a noise directivity, evaluated at a given emission instant, to a set of noise relevant parameters. This can be obtained using the second SELENE main functionality: backward propagation. Here SELENE is used in order to remove all propagation effects from flight-test-microphone signals in order to characterize the noise emission of the helicopter at a given time with respect to the selected noise relevant flight parameters.

The microphones layout used during the PAVE tests counts 43 microphones placed on grass or on

5

concrete, all set head down. The layout allows to collect the instantaneous noise emission with a good directivity coverage when the helicopter is approximately above the center of the microphone carpet.

In order to remove effects of propagation, the noise (narrow band spectra) collected at different reception times is back-propagated onto a fictitious sphere centered at the rotor hub with radius 1 m. In the backward propagation functionality, we assume that the atmosphere is at rest and homogeneous (humidity 80%). As in forward propagation, atmospheric absorption, spherical attenuation, Doppler effect and ground reflexion are modeled, but this time removed from the microphones signals.

In order to avoid spurious amplification of background noise, especially at high frequencies, where the absorption to compensate is the highest, ground sound tone levels smaller than a fixed background noise threshold are set to zero.

2.2. Correlation between torque and noise

As explained in [6], the emission of noise seems to be highly dependent on the engine torque or engine torque ratio relative to a nominal torque value. As the engine torque ratio is displayed on the control panel of each helicopter, this dependency makes it possible to pilot quietly on the basis of targeted torque values as explored in [6]. This dependency was found/proven in 2008 after the optimization method based on the 3 previously mentioned noise relevant parameters had been set and has therefore no direct influence on the optimizations presented in this paper. However it is interesting to see which torque ranges identified as quiet the optimizer tends to exploit, in order to understand how the optimizer works and to get new information to develop further torque targeted flying procedures.

Fig. 3 shows the contour diagram of the averaged dBA levels on spheres with respect to horizontal velocity and calculated engine torque ratio. The diagram is drawn starting from roughly 7000 spheres resulting from the PAVE 2004 flight tests. Above 45% torque (region A), for almost all speeds, the spheres are in the blue region, relatively quiet. For lower torques, it seems that the noise radiation also depends on the horizontal velocity with respect to air. As the speeds above 100 knots are not well accepted for descents as they must be followed by strong decelerations, only regions B, C and D show exploitable quiet descents.

The engine torque ratio indicated to the pilot during the PAVE 2004 flight tests has not been measured. The torque on each engine has been measured and the engine torque ratio can be easily deduced from these measurements. However there was a problem in these torque measurement which could not yet be corrected. As all the tested flights were simulated

with HOST afterwards to get the value of *RmAlpha* and *RmCT*, the torque on the main and tail rotor was available form the simulation. The engine torque ratio was then evaluated using the following formula:

$$1) \; \text{Torque\_ratio}_{Engine} = 100 \frac{(\Omega_{MR} T_{MR} + \Omega_{TR} T_{TR})}{(0.97 * 2 * T_{EN} * \Omega_E)}$$

where Ω_{MR} and Ω_{TR} are the main rotor and tail rotor rotation speeds (assumed to be constant), T_{MR} is the main rotor torque (only the component in shaft direction), T_{TR} is the tail rotor torque (component in shaft direction), and Ω_E the engines rotation speed (assumed to be constant). 0.97 is assumed to be the value of the gearbox efficiency. T_{EN} is the nominal engine torque.

At the time we used this formula, we had no information about the real values of engine torque ratio, and thus could not verify that its use with the HOST computed rotor torques provided the correct value. Negative engine torque values were obtained, which was not physically possible. Therefore the results have been shifted so that they all be positive. All the engine torque ratio values presented in this paper, including the one on Fig. 3, were obtained like this (HOST torques in Formula 1 + shift by 17%).

Due to those uncertainties in torque evaluation, various values of minimum torque were used as constraint in the optimization process in order to simulate various margins to autorotation.

We could observe recently that the evaluation of torque ratio as performed in this paper is still not well matching the engine torque ratio displayed to the pilots. Therefore do not use the values presented here as guidelines to the pilots. The trends are correct but not the absolute values.
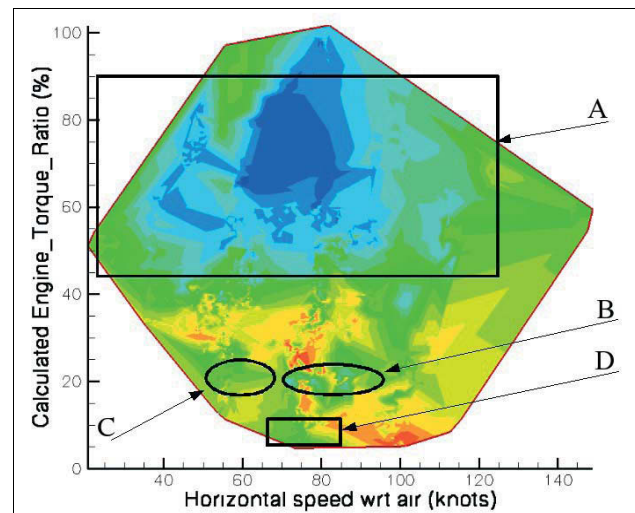

Fig. 3: Average dBA levels on spheres of radius 300 m, as measured in 2004, versus horizontal velocity with respect to air and versus engine torque ratio.

6

3. Optimization parameterization and setup

This section describes how the EC135 landing flight procedure optimization was constructed. We remind that we used the ModeFrontier [7] commercial optimizer with SELENE (forward propagation functionality) that calculated the noise generated by each trial procedure. Each iteration of an optimization refers to a landing procedure trial: the optimizer sets the way points of a new trajectory and a SELENE forward propagation calculation is automatically launched.

3.1. Definition of the S Coordinate System

A ground-fixed direct coordinate system called Simulation coordinate system S is frequently used for SELENE variable definitions. It is defined in the Friendcopter-dictionary. The axis $S3$ is vertical, upwards, the two other axes are horizontal. $S1$ represents the main flight direction. The origin SO is on the vertical projection of the nominal path on ground. For the present simulations SO and the landing point are identical.

This S coordinate system is used to locate the helicopter as well as the microphones.

3.2. Procedure parameterization

The Friendcopter partners planned to optimize landing flight procedures for 3 types of helicopter (EC130, A109 and EC135) and agreed to set common boundary conditions of the flight procedures. The agreed initial condition is an horizontal flight at 100 kts and 1000 ft above ground, at 5 km from the landing point. The final condition was hover slightly above the landing point, the final landing being left to the pilot and not being part of the optimization.

Each EC135 simulated procedure is assumed to be contained in the vertical plane $(S1,S3)$. No 3D trajectory were simulated, even if the computation chain allows it. This would have added too much parameters to the optimization, yielding very high convergence times, not compatible with the available time before the planned validation tests.

For all present EC135 optimized procedures, there were always 7 way points (or control points). Recall that the way points are the basic definition of a flight procedure with respect to ground. They define positions and values of the norm of the helicopter velocity with respect to ground at these positions.

The two first way points were always located 5100 m and 5000 m from SO (landing point) along $S1$. The altitude (HO_S3) and velocity norm ($NormVHO\_S$) was always the same on the two first points, in order to simulate a steady horizontal flight: 304.8 m (1000 ft) for incoming altitude (HO_S3), and 51.44 m/s

(100 kts) for incoming speed ($NormVHO\_S$).

The last way point is fixed and simulates the helicopter hovering above $S0$. Its altitude HO_S3 is 5 m (landing gear nearly 2m above ground).

Concerning HO_S2, its value is maintained to 0 m for all way points. All these constraints yield 12 optimization parameters: 4 representing HO_S1, 4 representing HO_S3, and 4 representing $NormVHO\_S$.

HO_S1 (m)	HO_S2 (m)	HO_S3 (m)	NormVHO_S (m/s)
-5100	0	304.8	51.44
-5000	0	304.8	51.44
free	0	free	free
free	0	free	free
free	0	free	free
free	0	free	free
0	0	5	0.1

Table 1: Coordinates and speed norm of the 7 way points for a typical optimization.

These parameters respect the Friendcopter agreed boundary conditions. Later, we also set free the incoming altitude and velocity, but still keeping their respective values identical for the two first way points, simulating a procedure starting with steady horizontal flight. This yielded optimizations with 14 parameters.

As explained in Section 1.3 we chose to simulate only flight with zero side-slip angle *beta*. In order to achieve that, the heading angle *psi* is adjusted in order to maintain *beta* = 0 all along the procedure, particularly when lateral wind is simulated.

3.3. Atmospheric conditions

The simulated atmosphere is an uniform one, with 80% of relative humidity and a temperature of 285.10 K.

Wind was simulated in HOST. That is to say that the relevant flight dynamics parameters have been calculated taking simulated wind into account. Nevertheless, as no ray tracing was implemented within SELENE at the time the optimizations were made, and as this step can be time-consuming for purposes like optimization, the wind and temperature gradients were not taken into account concerning sound propagation.

3.4. Simulated microphones field

The 77 simulated-microphones setup is shown on Fig. 4. Its length along $S1$ is 6000 m and its width along $S2$ is 4000 m. The difference in microphone density along $S1$ and $S2$ is refers to the difference in expectable SEL gradients in those directions.

For the EC135 optimizations we simulated an homogeneous ground with very high impedance (*sigma = 200000 kNsm^{-4}*, corresponding to a planar and infinite concrete-ground), although it would have

7

been less time consuming not to take into account ground reflection. Indeed, with such ground flow resistivity values, the ground reflexion spectrum is almost flat with value +6 dB, thus not changing the optimization result. All simulated microphones are placed 7 mm over the ground. This will later allow a validation with the microphones installed in the same manner on the runway, during flight tests.
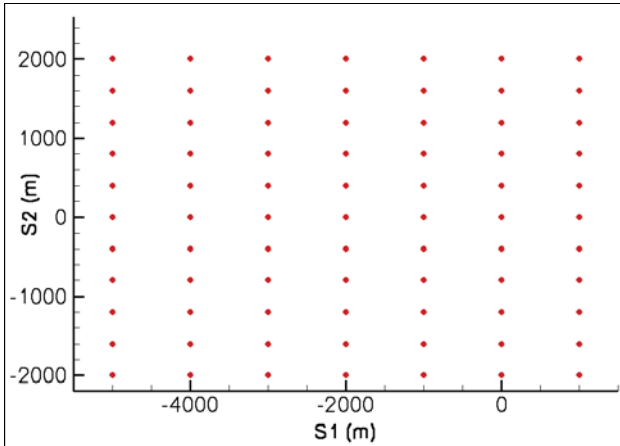

Fig. 4: Simulated microphones setup for the NAFP optimizations.

3.5. Cost function

The chosen cost function to minimize is the **S**ound **E**xposure **L**evels (SEL) average over the whole simulated microphone area. This is performed by a SEL dB averaging over all 77 simulated microphones as explained in Cost Function A below. *SELi* characterizes a whole procedure noise on a given microphone *i*. Using an energetic averaging as shown for Cost Function B is rejected as it would tend to make the optimizer minimize only the levels where they are the strongest (under the helicopter path and particularly at landing point). The choice of SEL as a metric was specified in the Friendcopter project.

$$2)\ Cost\ function_A = \frac{1}{n_{microphones}} \Sigma_i\ SEL_i$$

$$3)\ Cost\ function_B = 10 \log_{10}(\frac{1}{n_{microphones}} \Sigma_i 10^{\frac{SEL_i}{10}})$$

However this metric is not so well adapted to annoyance quantification. Indeed we could notice during validation flight tests that there were often differences in SEL ranking and subjective perception ranking. It thus seems important to use a more human representative metric for future noise footprint minimizations.

3.6. Optimization algorithm setup

The used algorithm in ModeFrontier is the Multi-Objective Genetic Algorithm II (MOGA-II), even if

only one cost function is used. Generational evolution was used, that is to say that all generations were fully described one after another. The generation size varied from 50 individuals, for the first optimizations, to 500 for the latest. First generation was randomly defined. Later in the process, we included some former results in new optimizations first generation for faster convergence.

- Probability of cross-over is set to 0.85: this is the probability of an individual to be defined by parents recombination.

- Probability of mutation is set to 0.1: this is the probability of an individual to be randomly changed.

- Probability of selection is set to 0.05 : this is the probability of an individual not to be changed from one generation to another.

- Elitism is enabled: the best solution of each generation is always transmitted to the next one.

A practical feature of ModeFrontier called adaptive evolution was also used in several of our optimizations. If one looks at Fig. 5, one can see among the points which represent fully calculated procedure, a green curve giving the cost function gliding average (on the last 100 successful iterations) along increasing iteration ID. The curve globally decreases roughly up to ID 10000. It seems that a local minimum is found there. At this point the average function increases instead of staying constant. This is due to the fact that the optimizer
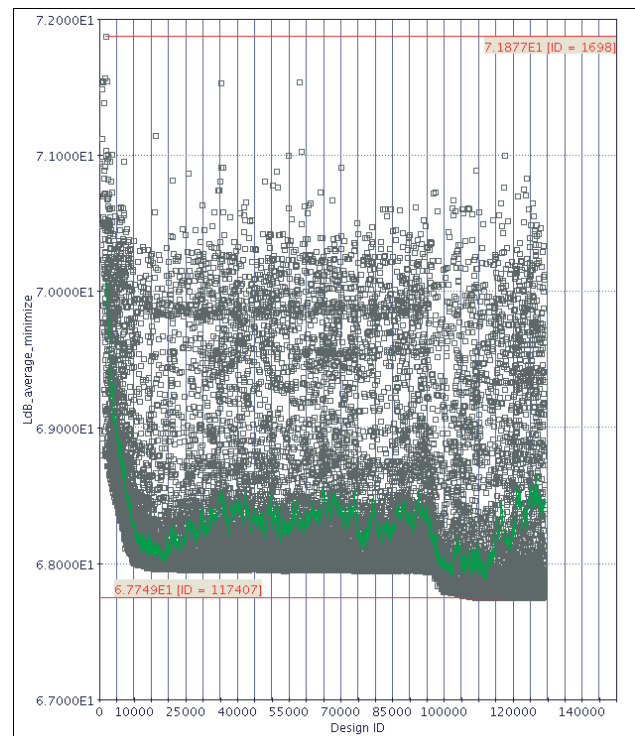

Fig. 5: Convergence of Optimization 53 - each point represents a fully calculated procedure.

8

increases its mutation ratio in order to find a possible other relative minimum (thus adapting the evolution). A newer minimum is then found roughly at iteration ID 100000.

It is of course never possible to know if the best design of the last computed generation is the global optimum. The choice to stop an optimization relies on the engineer. When we began to process such optimizations at DLR, they were performed on a single processor PC, yielding high calculation times. Then the SELENE computation chain was installed on the DLR Gauss cluster, and launched on more and more processors, that simultaneously evaluated designs. This explains why the first optimized procedures are deduced from relatively few iterations (approximately 1500 for the first ones, taking a whole week of calculation on a single computer).

We are now able to process an optimization on 32 processors in parallel, calculating 80000 iteration in 48 hours. When one looks at a cost function of such an optimization (see Fig. 6), it becomes clear that there are local minima in the cost function. That is to say that some of our optimizations, if not all, do not correspond to the global optimum. The only way to to get surely the global optimum would be to perform an exhaustive research, that is to say to test all the possible designs, which is impossible. We pushed the research to the limit of our reserved calculation capabilities for this study.

Nevertheless, some interesting trends were underlined during all these optimization processes (see Section 4), even if they possibly did not fully converged. Moreover, these trends were validated during dedicated flight tests (see Section 5).

3.7. The Reference Procedure

A reference procedure, including the noise certification 6 deg. 65 kts descent, was designed too, in order to quantify gains of the optimized flight
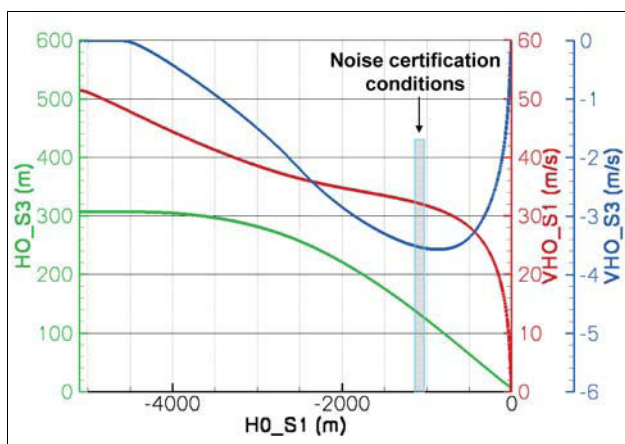
Fig. 6: Description of the Reference Procedure 7, a rather conventional landing, crossing the noise certification conditions.

procedures. It respects the Friendcopter agreed initial and final flight conditions and is close to current conventional landings. It is illustrated on Fig. 6. This reference procedure is relatively smooth, and DLR pilots consider it as easy to fly. It has been intensively flown during flight tests for different wind and temperature conditions. This procedure is known to generate some BVI noise, but nevertheless does not represent the noisiest procedure conceivable. Its SELENE simulated noise footprint is shown in Fig.7.
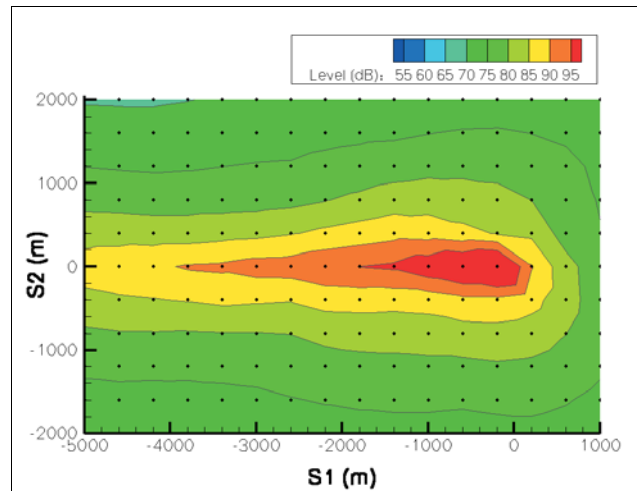

Fig.7: Simulated Sound Exposure Level of Reference Procedure 7.

4. Optimized procedures and their trends

This section describes some representative optimization results which were calculated according to different sets of masses, winds and constraints.

As we obtained continuous feedback from the pilots, the SELENE flyability module was improved all along the optimization study to add more and more constraints to the optimizer. This explains why some of our first-calculated procedures had to be hand-adapted after first flight tests, in order to be completely flyable.

4.1. Optimized Procedure 6

Procedure 6 (see Fig. 8) results from one of the first performed optimizations and took approximately 1500 trial iterations running on a single processor. The boundary conditions are the Friendcopter ones. No wind was simulated. In order to keep a margin to autorotation, no value of calculated engine torque ratio (see section 2.2) below 8% was allowed.

The result shows a procedure beginning with a climb from 300 m altitude up to 400 m. During the climb phase the helicopter speed remains constant at 100 kts, but for this optimization 100 kts was set as maximal speed constraint. Approximately 2000 m before the landing point *S0*, the helicopter begins its descent to the landing point. In parallel, the horizontal speed decreases. Torque goes down (to its 8% limit), as well as aerodynamic slope *gammaA*. Again the optimizer attempts to avoid the noisy zone of the torque value, going in D region of Fig. 3. At the very end of the procedure, the slope and torque go up rapidly which corresponds to flare and power recovery to prepare hover. This leads to some noise increase around the helipad (see Fig. 10), as the noisy torque zone is crossed another time. Fig. 9 shows the simulated SEL of this procedure. To get a better resolution, the procedure propagation was re-calculated, this time using 178 regularly-spaced simulated microphones, as for simulation of Reference Procedure 7 (see Fig.7). SEL of Procedure 6 is asymmetrical, the noise being slightly higher starboard, which corresponds to the advancing blade side. On Fig. 10 one can see the predicted noise reduction of Procedure 6. It is mostly concentrated under the helicopter path, approximately 2000 m before the landing point, and can reach 12 dB SEL. The noise reduction during climb might be attributed to the increasing distance to ground. But this effect, approximated by spherical spreading difference represents only 2.5 dB for this
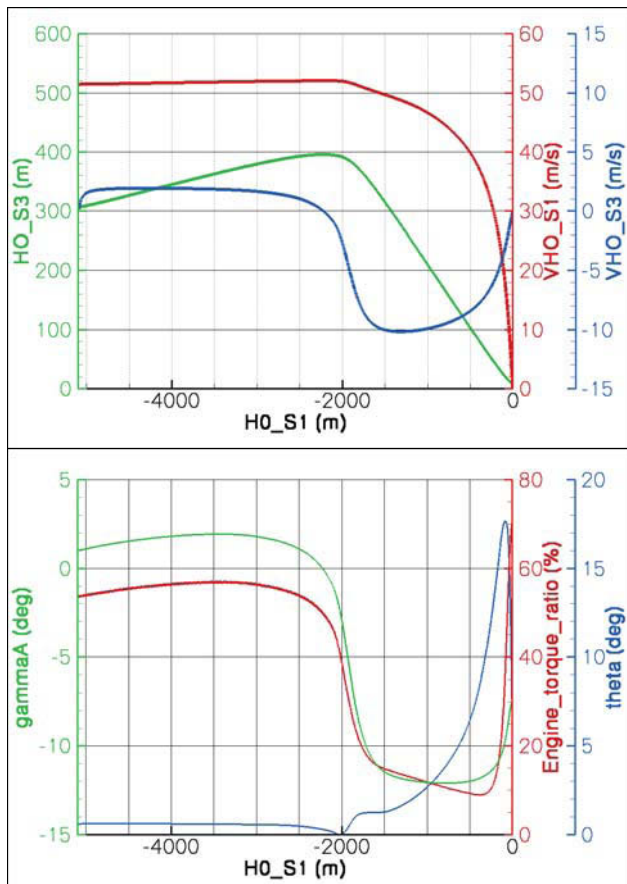
procedure. The remaining and consequently main noise reduction comes from the reduced noise emission, due to the change in flight conditions. Indeed, the climb allows to increase torque at given horizontal speed, producing in this case a quieter emission (see Fig. 3) which can be explained by the quick convection of blade tip vortices significantly below the rotor disk, thus avoiding BVI.

Attitude angle theta reaches briefly high values at the end of the procedure, leading to a difficult flyability. Nevertheless, this is not of major acoustic relevance, as the noise reductions are clearly located far before the landing point, and as minimizing the noise on the helipad is not a major concern. This typical optimized high *theta* values can be explained by the fact that the optimizer, after flying a quiet procedure, tends to make the helicopter land as quickly as possible to lower the SEL which is a time-integrated metric. The solution applied to make this procedure more flyable was to shift it 100 m away from the landing point and to provide thus the pilot 100 m more to perform the flare. This resulted in Procedure 46.
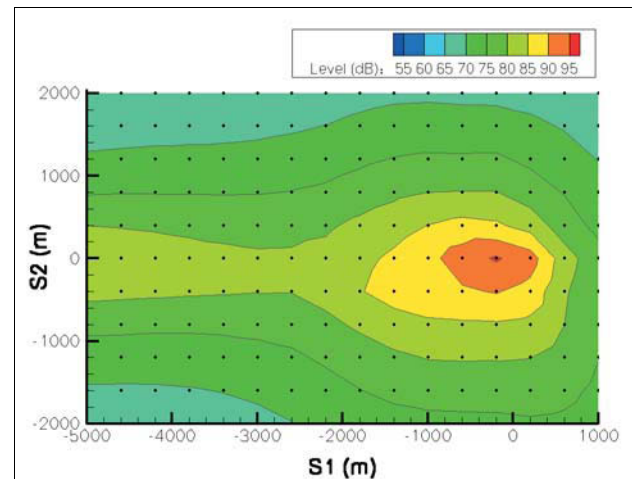

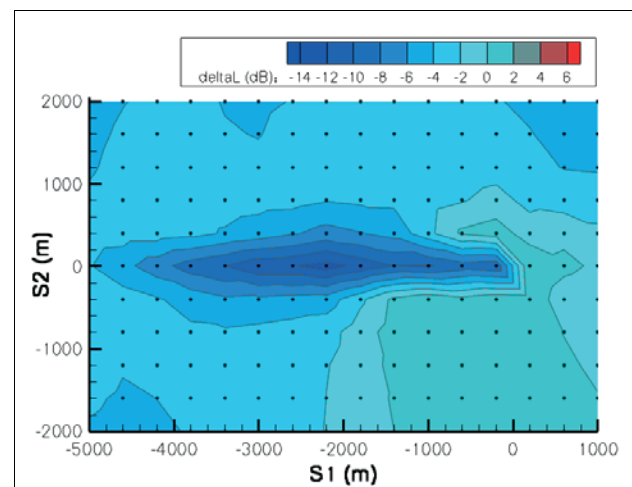Fig. 9: Sound Exposure Level of Optimized Procedure 6.

Fig. 10: Difference of SEL levels between Optimized Procedure 6 and Reference Procedure 7.

Fig. 8: Procedure 6 .

10

4.2. Influence of engine torque ratio constraint – Optimized Procedure 11

After feedback from pilots concerning Optimized Procedure 6, it was decided to increase the lowest torque limit to 13% to avoid autorotation. Indeed, during preliminary flight tests, pilots said that such a procedure is quite difficult to fly, as it is close to autorotation (later, after more training it was judged flyable). This new constraint yielded Optimized Procedure 11. This time the optimizer did not go until the torque limit, the lowest torque value upon the procedure being approximately 18.5 %. This yields a more flyable descent with a maximum descending speed of roughly -7 m/s.

Again, the optimizer tends to make the helicopter land very quickly at the end of the procedure, yielding high *theta* values (up to approximately 21 deg). As one can see on Fig. 12, the gains before landing point are not as important as for Procedure 6 (only 7 dB SEL reduction 2000 m before the landing point). Moreover, one can see some worsening on the advancing blade side, which could be explained by uncanceled BVI (which was also noticed during flight tests). Indeed, the optimizer used region B for the descent phase (see Fig. 3), which is quite thin, and therefore it is difficult to remain quiet while flying this region.

Some gains are also obtained beyond the landing point, in a not overflown region. Indeed, the

helicopter, being already within the noisy torque region, does not have to cross it totally to land. This can also be explained by the high *theta* values, yielding a strong deceleration, which decreases the landing time and thus the SEL at the end of the procedure. Nevertheless, flying such a fast flare is difficult. A flown theta higher than the prescribed one means a loss of visibility whereas a lower value means a landing point overshooting.
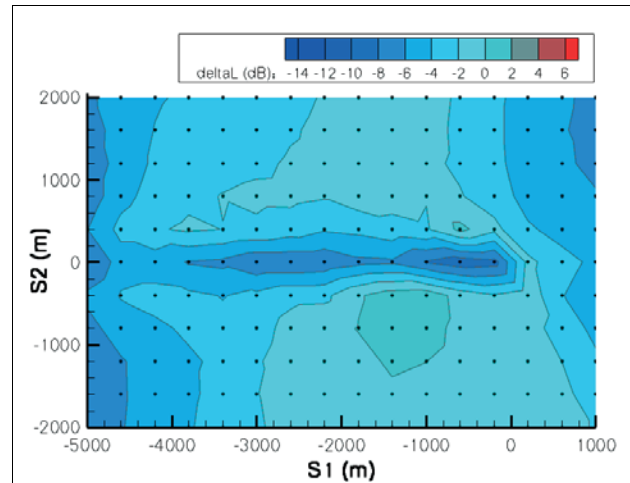

Fig. 12: Difference of SEL levels between Optimized Procedure 11 and Reference Procedure 7.

4.3. Influence of side wind – Optimized Procedure 10

We then wanted to quantify the effect of wind on the optimizations. A situation with no wind is indeed quite rare in real operation. But for a given wind, the pilot can choose its flight direction with respect to wind direction, however rejecting flight directions leading to tail wind component, for safety reasons.

Procedure 10 was optimized taking into account a wind coming from port (left side). We use a standard wind profile varying with altitude. Only horizontal wind is taken into account. Its speed is roughly 5 m/s at 10 m height and 15 m/s at 300 m height. The torque constraint (higher than 13%) is the same as for Procedure 11.

Procedure 10 is found relatively close to Procedure 11 (see Fig. 13), and especially the torque that tends to go into the same region (see Fig. 14). The horizontal speed remains here almost constant until the beginning of descent, whereas for Procedure 11 a slight deceleration occurred. Fig. 16 shows that the noise reduction of Procedure 10 is slightly higher than for Procedure 11. In fact, even when simulated without lateral wind, Procedure 10 gives a similar noise reduction than with lateral wind. This tends to prove that a lateral wind does not affect the optimization result for this type of procedures (with torque margin to autorotation).
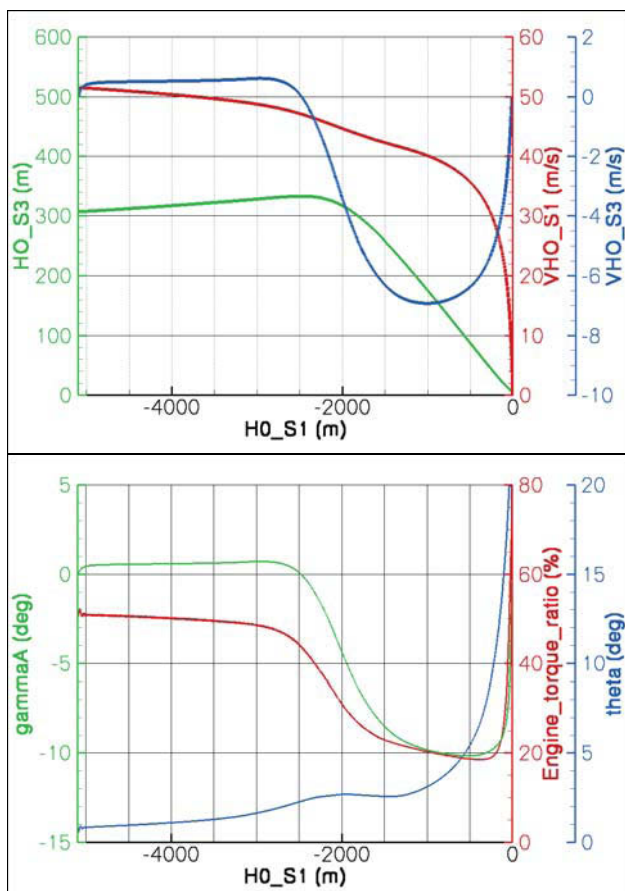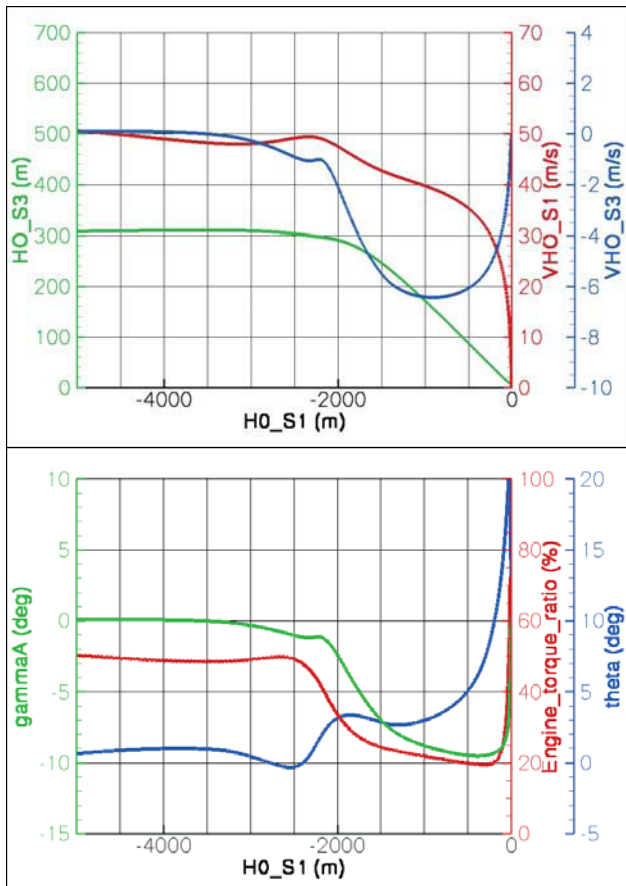

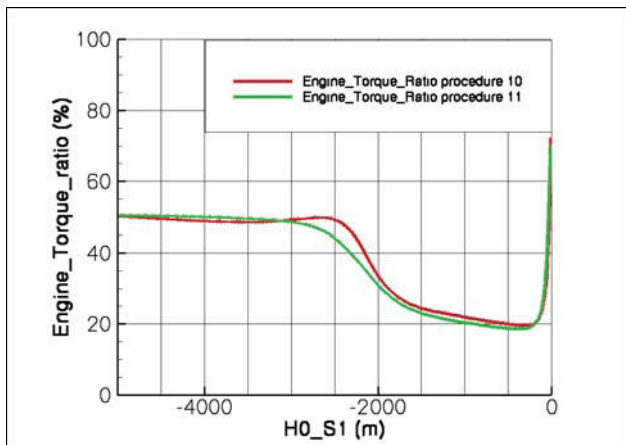*Fig. 11: Optimized Procedure 11.*

Fig. 13: Optimized Procedure 10.

Fig. 14: Comparison of Procedure 10 and Procedure 11 engine torque ratios.

4.4. Influence of the helicopter mass – Optimized Procedure 53

We also tried to quantify the influence of the helicopter mass on the optimization result. The lower torque limit is here again 8%, as for Procedure 6 (indeed with some training the pilots found Procedure 6 flyable). The default helicopter mass used for the optimizations was 2500 kg. Here for Procedure 53, the mass of 2700 kg was chosen.
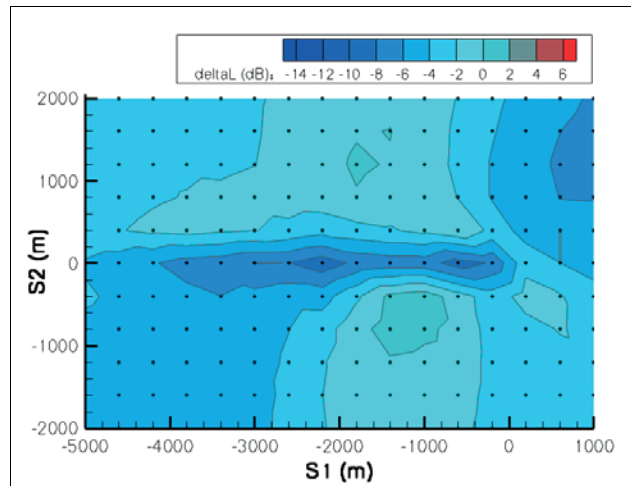

Fig. 15: Difference of SEL levels between Optimized Procedure 10 and Reference Procedure 7.

Procedure 53 is shown on Fig. 16 and the comparison of its torque with the one of Procedure 6 is given in Fig. 17. Again the optimizer tends to avoid the noisy torque region. This procedure was calculated in 2009, using 32 processors on Gauss Cluster. Instead of roughly 1500 iterations for Procedure 6, we ran 130000 iterations. The convergence can be seen in Fig. 5. The optimizer configuration let this time the speed free up to 60 m/s (instead of 52 m/s previously). Moreover, some additional flyability constraints were in the meanwhile
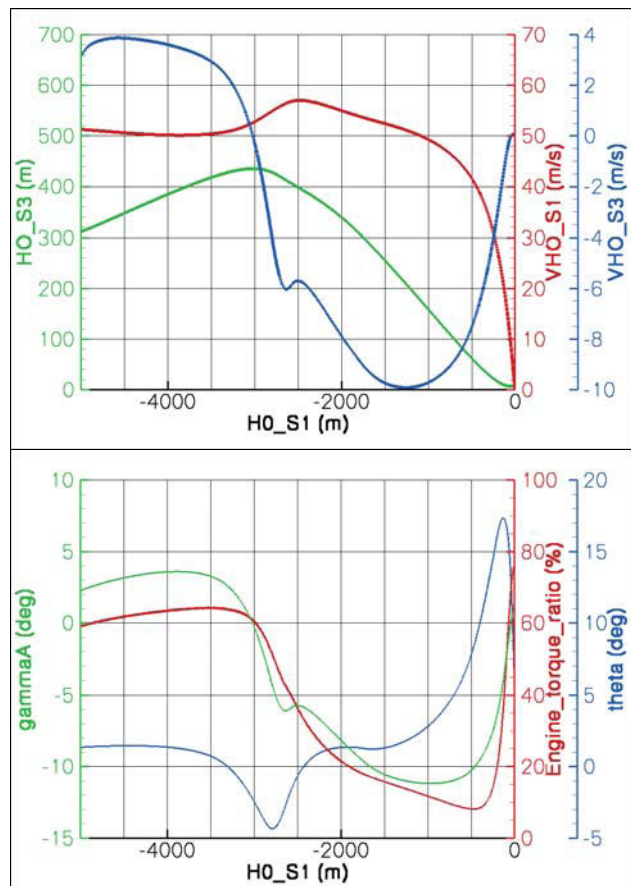
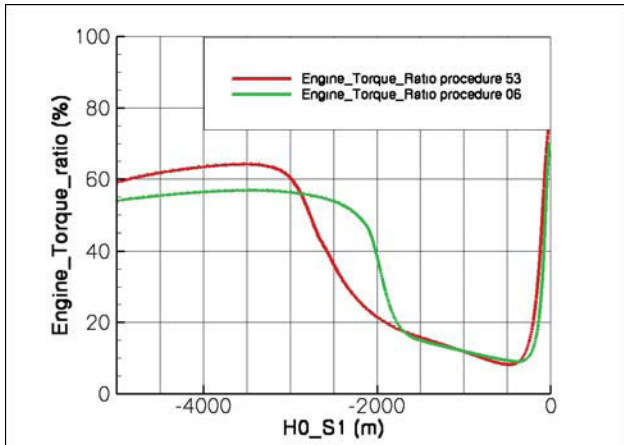Fig. 16: Optimized Procedure 53.

12

Fig. 17: Comparison of Procedure 6 and Procedure 53 engine torque ratios.

introduced within SELENE, including a control over the acceleration derivative. These are the reasons why the torque is higher than for Procedure 6 at the beginning of the procedure, and why it declines smoothly. Nevertheless, the trends of Procedure 53 and of Procedure 6 are similar, and so are their noise footprints. This tends to prove that the noisy torque region avoidance concept is valid for various helicopter masses and that an 8% mass increase has a small impact on the optimal procedure and on its resulting noise on ground.

4.5. Influence of a free incoming altitude – Procedure 34

Procedure 34 is the optimization result corresponding to the introduction of a new design parameter: the incoming height. Here the lower torque limit is 13% as in Procedure 11. Zero wind is simulated. Fig. 18 shows Procedure 34 and Fig. 19 the comparison of its torque evolution with the one of Procedure 11. The optimizer reduced the incoming altitude to roughly 210 m. This allows to increase the torque during the climb part up to 300 m. Then the helicopter goes in the same torque region as for Procedures 10 and 11.
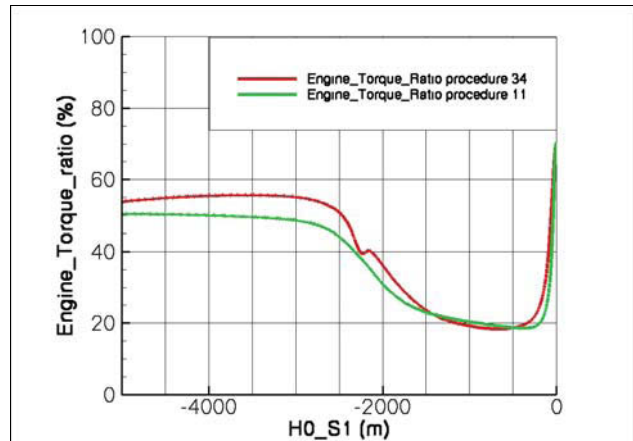
4.6. Influence of interpolation scheme – Procedure 63

The nature of the optimized trajectory is also influenced by the way SELENE is parametrized. Indeed, there are two available ways to interpolate the simulated emission sphere from the selected database-spheres at each time step. The first method consists in processing for each tone of the spectrum a weighted SPL dB averaging between the tones of the selected database-spheres. The second way is to perform a weighted average of the quadratic pressures for each tone. It has already

Fig. 18: Optimized Procedure 34.

Fig. 19: Comparison of Procedure 11 and Procedure 34 engine torque ratios.

been observed that the first method is more secure when one wants to simulate accurately a given procedure. Indeed, when one uses quadratic pressures, a possible overestimated value on one of the selected database-sphere (for example due to drastic brief background noise increase during measurement) can drastically influence the SPL level on the interpolated sphere, whereas with the dB SPL interpolation the influence is weaker. On the contrary, concerning optimization, it can be
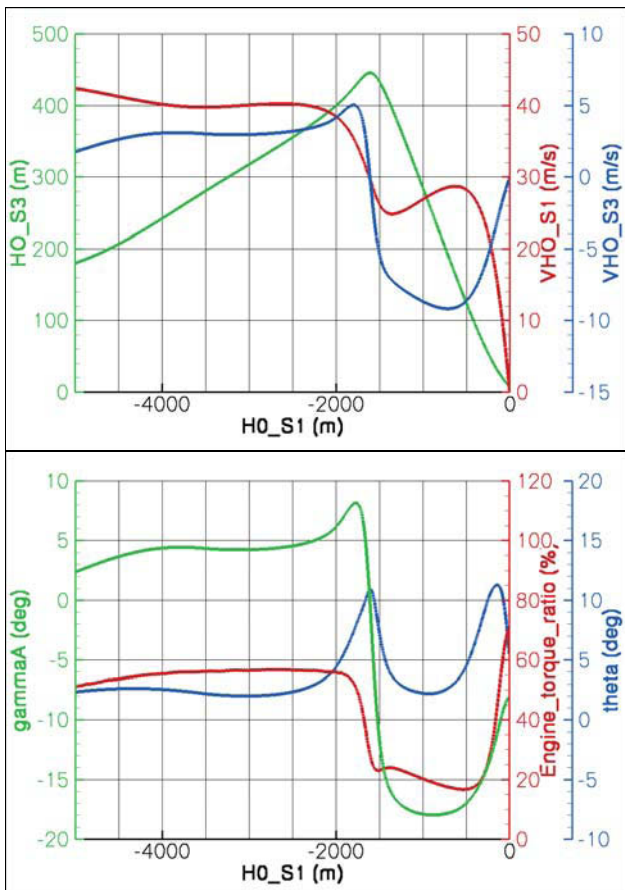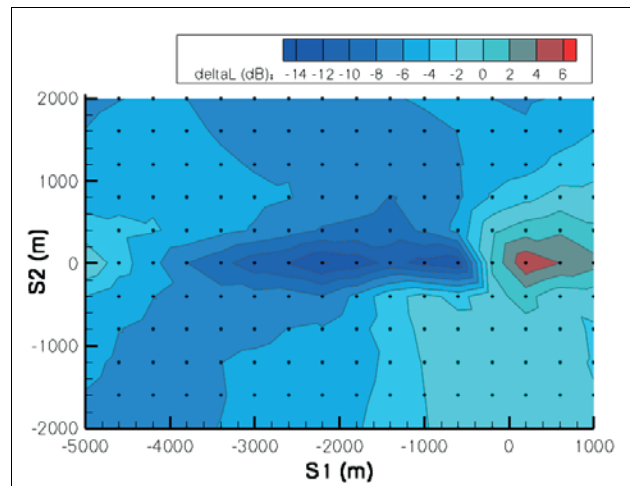
13

Fig. 20: Optimized Procedure 63.

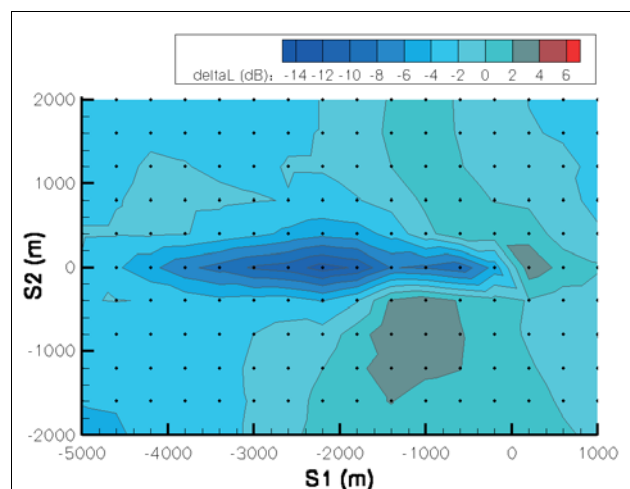Fig. 21: Difference of SEL levels between Optimized Procedure 63 and Reference Procedure 7.

Fig. 22: Difference of SEL levels between Optimized Procedure 63 simulated with additional headwind and reference Procedure 7.

interesting to use a quadratic pressure interpolation, in order to avoid too small quiet regions of the torque/velocity diagram (for instance region B on Fig. 3). Indeed when one of the selected sphere is in a rather louder area the interpolated sphere is loud and the optimizer searches for selected spheres all in a quiet area. Optimized Procedure 63 was calculated using such a quadratic pressure interpolation. Incoming altitude and velocities were also set free. Note that for this optimization the cost function was estimated in EPNL instead of SEL to better represent human hearing. Procedure 63 is drawn in Fig. 20. Its noise reduction in SEL compared to Procedure 7 is plotted in Fig. 21. During descent phase, the helicopter goes now in the C region of Fig. 3.

4.7. Influence of headwind on an optimized procedure

As for a given procedure (defined with respect to ground) headwind modifies *PmAlpha*, and thus the emitted noise, we wanted to test the robustness of one of our procedures to headwind. Fig. 22 shows the noise reductions of Procedure 63, flown with a simulated headwind, of about 5 m/s at 10 m height and 15 m/s at 300 m height. This is the same wind profile as for Procedure 10, but in another direction.

One can see that the noise reduction is clearly lower as for the no-wind case (Fig. 21). Worsening is also observed on the advancing blade side. This can be explained by the fact that this procedure uses the C region (see Fig. 3) to fly quiet. As a headwind yields an increase in horizontal velocity with respect to air, the noise emission is notably increased in this case.

From other optimizations not shown here we learned that procedures optimized with headwind are generally different from the procedures optimized with zero wind and that the noise reduction achieved tends to be weaker than with zero wind. As on the contrary, the impact of lateral wind on optimized procedures and on their noise reduction has been shown to be minor, choosing the landing direction so that the wind is rather lateral than frontal may produce acoustic advantages for quiet landing. However the wind effects should be investigated in a deeper manner once the ray tracing module will be coupled with SELENE, to account also for the large effects of wind on propagation.

14

5. In-flight validation

5.1. Flight test setup

This section describes how the calculated flight procedures were validated during a flight test campaign in 2008, on Cochstedt airport (Germany). The microphone layout was already presented in [6], and is recalled in Fig. 23. Recall that each procedure has to be flown twice, the second time with a longitudinal shift, to generate a 6 km long measured footprint.
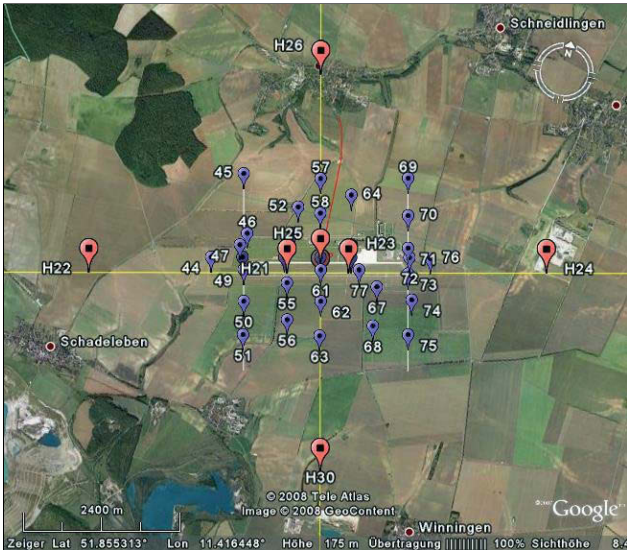

Fig. 23: Cochstedt 2008 microphones layout. The violet points represent the microphones positions, and the orange points the possible landing points.

The reference and optimized procedures were indicated to the pilot on a visual display especially developed for this purpose in Friendcopter. This display is presented in [6] with its particularities making him suited for the noise abatement procedure flying without noisy unwanted theta oscillations. At the moment of the validation flight tests it was ready to be used.

5.2. Final procedure adjustments

As our optimized procedures benefited from the pilots' feedback, several procedures were adjusted by hand to achieve a better flyability. Of course, SELENE was also launched on the adjusted procedures to check that the modification did not impact much the optimized noise reduction.

For example, we remind that Procedure 46 was generated from Procedure 6, by providing a 100 m horizontal extension at the end of descent to allow an easier flare. This eliminates the risk to overshoot the landing point if the glide slope flown during descent is not completely as steep as the simulated one, or if the conversion from climb to descent occurs a little bit to late.

As demonstrated in [6], the side-slip angle beta has a high potential of Fenestron excess noise avoidance for low torque descents. This is the reason why beta values from -15 to -25 deg were introduced in the flight test during the descent phase of each optimized procedure.

5.3. Limitation factors for the present validation extent

At the time we conducted the flight tests, some recent procedures were not available. This explains why Procedures 53 or 63, for example, are not yet flown and validated.

The results from the flight test campaign are not yet fully post-processed. This section aims to show that some trends underlined during the calculation process were confirmed in flight. Nevertheless, many factors still have to be taken into account in the SELENE simulation in order to properly validate this computation chain versus the flight tests :

- Only few microphones were directly located upon concrete (typically the ones under helicopter path). Many microphones were located in fields, on microphone plates or on tripods, whereas for the present SELENE computation the ground was assumed flat, homogeneous and with infinite impedance.

- The test field was not completely plane (until 15 m height difference for some outer microphone positions). This should also be modeled in the near future, although the introduced error remains much smaller than 1 dB and only for the concerned microphones.

- The wind and temperature gradients were not taken into account in the propagation simulation. Even if a high-quality meteorological measurement was performed, its data are not post-processed yet. That is to say that we compare here procedures which were simulated without wind gradients and actually measured procedures with sometimes wind gradients.

- The helicopter mass in the SELENE calculations can differ from the actual mass during flight. As mass may have an effect on noise relevant parameters the comparisons should be performed with identical masses.

- And, of course, the procedures could not be flown exactly as calculated. In the future we will directly simulate in SELENE the procedures as they were flown.

It is nevertheless already possible to compare the predictions and measurements corresponding to the microphones placed on the runway (*i.e* on concrete), which were directly under the helicopter path.
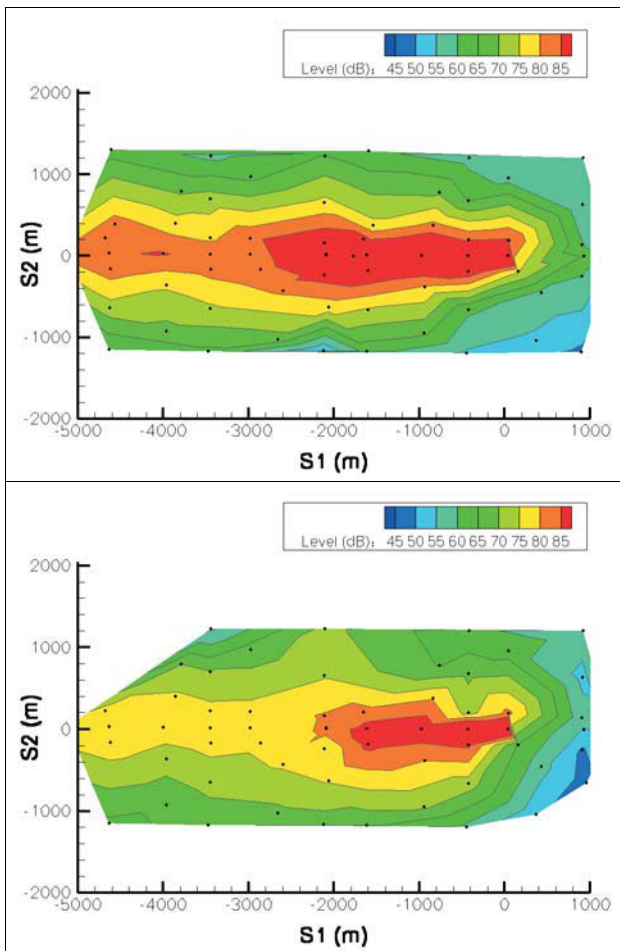
Fig. 24: Reference Procedure 7 and Optimized Procedure 46 measured SEL contours.

Before focusing on those runway microphones, we can check the noise footprint evolution. Fig. 24 shows the measured SEL contours for Reference Procedure 7 and for Optimized Procedure 46. Note that the color step corresponds to 5 dB SEL. The low noise levels on side are slightly increased in Procedure 46 but the highest noise levels under path of Procedure 7 are considerably reduced so that the 80 dB and 85 dB contour areas are reduced by about 60% from Procedure 7 to Procedure 46.

5.4. SELENE and optimized procedures validations

Fig. 25, Fig. 26, and Fig. 27 present comparisons between flight test results and SELENE calculations, with all the approximations mentioned before. The agreement SELENE / flight tests is satisfactory.

In particular, Fig. 25 shows that, taking into account all the assumptions listed before, the variability between two measurements of the same procedures has the same order of magnitude as the interval between calculations and measurements (roughly 4 dB, except for the 2 last points). The not so good agreement at the microphone positions at 0 m and at roughly + 1000 m along $S1$ can be explained by the

fact that it was difficult to fix the dBA integration time to calculate the SEL as the helicopter stops in hover. As the SEL level depends then directly on integration time, this can have a notable effect on the measured level. Furthermore, at the end of the procedure the altitude is quite low. That is to say that the emission is highly extrapolated on the sphere.

Fig. 26 shows an irregularity in the measured SEL of Procedure 11, roughly 1500 m before the landing point. This can be explained by the fact that the descent part of such a procedure is flown in region B (see Fig. 3). As this region is relatively small, and surrounded by noisy flight conditions, it is thus quite difficult for the pilot to remain within it. It could also be noticed from hearing that Procedure 11, while being globally quieter than the reference, shows some incursions in BVI.

Nevertheless, the relatively good agreement between measurements and calculations as shown on the 3 last figures shows that SELENE is able to well model various complete EC135 procedures, all going through various flight conditions. We remind that we used here our 2004 flight tests aeroacoustic database to simulate the flights tested in 2008.

Fig. 28 contains only measurement results. As predicted during the optimizations, in the domain from 3000 m to 500 m before landing point, the flight tested optimized procedures show a noise reduction from 8 to 12 dB compared to the Reference Procedure. Among the already tested optimized procedures Procedure 46 is the one that produces the highest noise reduction. Its noise footprint (reminded in Fig. 24) and the comparison between flown and prescribed flight parameters have already been presented in [6].
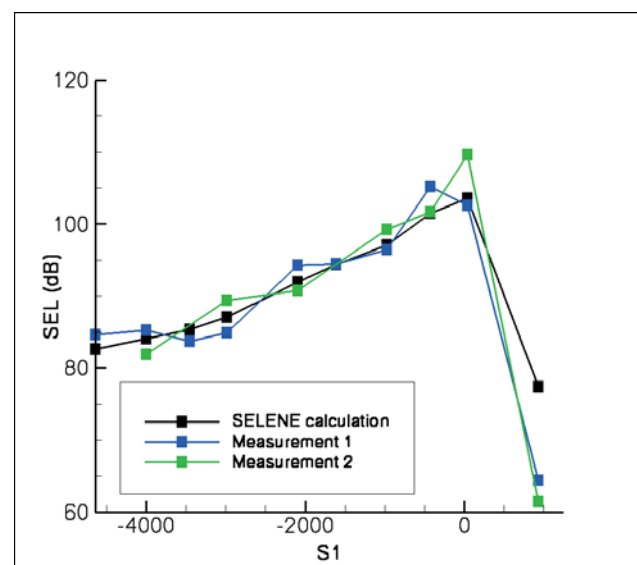

Fig. 25: Comparison SELENE-flight for Procedure 7.
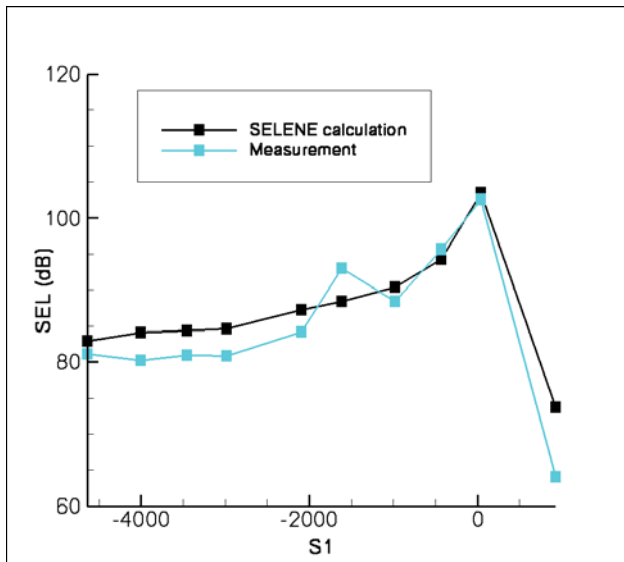
16

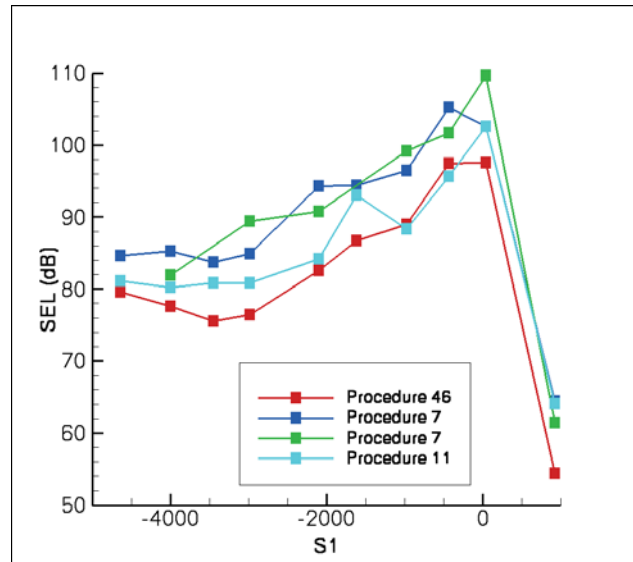Fig. 26: Comparison SELENE-flight for Procedure 11.

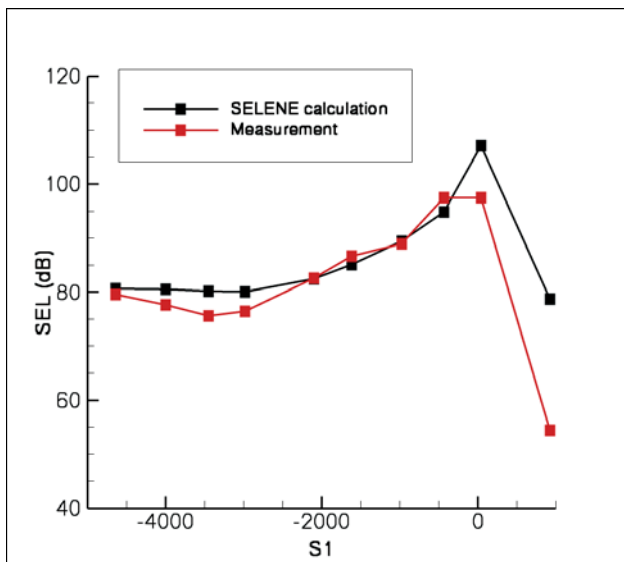Fig. 28: Comparison between the measured procedures.

Fig. 27: Comparison SELENE-flight for Procedure 46.

5.5. About the pilots and passenger acceptance of the optimized procedures

The pilot could well and with a good repeatability fly the optimized procedures after some training. It is true that several descent phases are close to autorotation. However the engines are running all the time and power is available at any time to interrupt the descent if required. The optimized flight procedures do therefore not present the danger of the emergency autorotation landing performed in case of engine failure.

Concerning the passengers, the only discomfort may be felt when the transition from climb to descent is made quickly (to avoid totally BVI noise occurrence) and with the simultaneous side-slip occurrence. After some of such transitions passengers get used to it. The flight with large side-slip, and its resulting roll, which is large with the high landing gear option, may worry some passengers. The Fenestron noise excess avoidance which is demonstrated in our tests thanks to a large side slip, could be obtained identically with zero side-slip provided the helicopter be designed with a dedicated controlled flap on the tail fin.

The sink-rate limitation to 1000 ft/min generally set in civil aviation is violated with for example Procedure 46, descending at 2000 ft/min. The limitation to 1000 ft/min is mainly due to the problem of pressure compensation in the middle ear. DLR tests were made with 1 pilot and 4 passengers in a BO105 and showed that when descending starting from 2000 ft to ground at 2000 ft/min, 2 of the 5 helicopter occupants effectively noticed ear pressure problems. However when starting only at 1000 ft height, as for the optimized procedures, no occupant had problems with ear pressure compensation. Therefore the 1000 ft/min sink rate limitation seems not relevant for the present optimized flight procedures. During all the validation flight tests, pilots and flight test engineers never reported ear pressure compensation problems.

17

Conclusion and perspectives

This paper presents progress achieved in the optimization of noise abatement flight procedures for an EC135.

– The SELENE calculation chain, able to model arbitrary flight procedures including maneuvers and wind, starting from a database, here resulting from PAVE 2004 flight tests, has been implemented in a genetic optimization loop. It uses the flight dynamics simulation code HOST and checks the flyability, safety and comfort of the simulated flight procedures which are generated starting from way points and prescribed velocity at those points. The parameterization and setup of the optimizer for the optimization of noise abatement EC135 landing procedures whose paths are in a vertical plane has been described. Concerning the iteration number limitation for example, it has been shown that it is worthwhile to run more than 100000 iterations.

– A series of such optimizations of landing procedures has been conducted. Depending on the parameters fixed in terms of mass, wind, torque limitation, flyability constraints, initial conditions on height, or SELENE parmetrization, the optimizer found out several noise abatement flight procedures. These procedures, when confronted to a torque/velocity diagram, show several strategies to achieve noise reduction. Noise reductions up to 10 dB SEL were predicted, compared to a reference procedure crossing the noise-certification descent-flight.

– The optimized procedures are rather insensitive to lateral wind component. However headwind can have an important impact. A variation of mass of about 8 % seems to not much affect the optimization results.

– Some of the shown procedures where validated in flight tests in 2008. The SELENE computations are in satisfactory agreement with the flight test results and the optimized flight procedures are rather well flyable.

– The flight tests confirm the predicted noise reduction by 10 dB SEL between 3 km and 1 km before the landing point.

Regarding these results, further activities have been planned at DLR in the noise abatement procedures design field.

The presented methodology is currently applied to the BO105 helicopter. Some variations on the optimization cost functions, for example, towards noise metrics closer to human hearing are also applied to the EC135. The resulting new BO105 and EC135 optimized procedures will be flight tested.

In the framework of the JTI Clean Sky it is planned to make additional developments towards the exploitation of noise abatement flight procedures in all-day operations.

Acknowledgments

Authors workshare

Frédéric Guntzer (at DLR since April 2007) : completion of HEMISPHERE 2 (coding of forward propagation, of a reflexion model for homogeneous ground, of an atmosphere table model, implementation of microphone plate correction, 2D triangulation on spheres, improvement of computation speed), construction of the spheres database, scripting and completion of the computation chain for the simulation of arbitrary flights using a flight test data base, automatic correction of the nose boom velocity measurement, introduction of the simulation chain in an optimizer, installation with parallelization of the optimization loop on the Gauss and CASE PC clusters, contribution to the definition of netCDF files, completion of flyability constraint coding, run of the noise footprint minimization for various conditions. Merge of all modules in a better rationalized and user friendly computation chain: SELENE.

Pierre Spiegel: setting in 2003 of the architecture of the methods employed in the DLR noise abatement procedure optimization, continuous development orientation based on physics, project leader for the helicopter NAFP development at DLR, flight test lead and design for PAVE 2004 and Friendcopter/PAVE 2008 and for their preliminary flyability tests, collecting of pilot feed back and flyability limits. Ideas of torque-noise dependency and of side-slip to eliminate Fenestron excess noise.

Markus Lummer: development of the flight procedure generation program based on Bézier cubic Splines and compatible with helicopter flight dynamics. Development of the Ray Tracing simulation tool to be coupled with SELENE.

Bibliography

[1] Le Duc A. ; Spiegel P., **Definition of Coordinate Systems and Variables for Aircrafts and Rotorcrafts, their Kinematiks, Dynamics and Acoustics**. "Friendcopter Dictionary" V12.3, 2008.

[2] Spiegel, P. ; Buchholz, H. ; Splettsloesser, W., **The "RONAP" Aeroacoustic Flight Tests with a Highly Instrumented BO 105 Helicopter**, 59th American Helicopter Society Annual Forum, Pheonix, Arizona, USA, May 2003.

[3] Yin, J. ; Spiegel, P. ; Buchholz, H., **Towards Noise Abatement Flight Procedure Design: DLR Rotorcraft Noise Ground Footprint Model and its Validation**, 30th European Rotorcraft Forum, Marseilles, France, September 2004.

[4] Pierre Spiegel, Heino Buchholz, Michael Pott-Pollenske, **Highly Instrumented BO105 and EC135-FHS Aeroacoustic Flight Tests including Maneuver Flights**, American Helicopter Society 61st Annual Forum, Grapevine, Texas, USA, June 1-3, 2005.

[5] Le Duc A.; Spiegel P.; Guntzer F.; Lummer M. ; Buchholz H.; Götz J., **Simulation of Complete Helicopter Noise in Maneuver Flight using Aeroacoustic Flight Test Database**, American Helicopter Society 64th Annual Forum, Montréal, Canada, April 26th – May 1st, 2008.

[6] Pierre Spiegel, Frédéric Guntzer, Anne Le Duc, Heino Buchholz, **Aeroacoustic Flight Test Data Analysis and Guidelinesfor Noise-Abatement-Procedure Design and Piloting**, 34th European Rotorcraft Forum, Liverpool, UK, 16th - 19th September, 2008. (Cheeseman Award Paper) Also presented at 65th American Helicopter Society Annual Forum, Grapevine, Texas, USA, May 27-29, 2009.

[7] ESTECO, **ModeFrontier v4**,http://www.esteco.com.

[8] Engeln-Müllges, G. ; Reutter, F., **Formelsammlung zur Numerischen Mathematik mit Turbo-Pascal Programmen**, BI-Wiss.-Verl., Mannheim/Wien/Zürich, 1991.

[9] Benoit, B.; Dequin, A.-M.; Kampa, K.; Gruenhagen, W.; Basset, P.-M. and Gimonet, B., **HOST: A General Helicopter Simulation Tool for Germany and France**, 56th American Helicopter Society Annual Forum, Virginia Beach, Virginia, USA, May 2000.